ARTICLES
https://doi.org/10.1038/s41593-018-0121-5
nature neuroscience

Myelin remodeling through experience-dependent oligodendrogenesis in the adult somatosensory cortex

Ethan G. Hughes[1,2,4*], Jennifer L. Orthmann-Murphy[1,3,4], Abraham J. Langseth[1] and Dwight E. Bergles[1*]

Oligodendrocyte generation in the adult CNS provides a means to adapt the properties of circuits to changes in life experience. However, little is known about the dynamics of oligodendrocytes and the extent of myelin remodeling in the mature brain. Using longitudinal in vivo two-photon imaging of oligodendrocytes and their progenitors in the mouse cerebral cortex, we show that myelination is an inefficient and extended process, with half of the final complement of oligodendrocytes generated after 4 months of age. Oligodendrocytes that successfully integrated formed new sheaths on unmyelinated and sparsely myelinated axons, and they were extremely stable, gradually changing the pattern of myelination. Sensory enrichment robustly increased oligodendrocyte integration, but did not change the length of existing sheaths. This experience-dependent enhancement of myelination in the mature cortex may accelerate information transfer in these circuits and strengthen the ability of axons to sustain activity by providing additional metabolic support.

Axons throughout the CNS are ensheathed by myelin, a form of insulation that accelerates action potential propagation and reduces both the energy expenditure required for transmission and the space necessary to assemble circuits capable of processing information with millisecond precision. The concentric layers of membrane that comprise myelin are formed by oligodendrocytes, each of which extends numerous processes to form discrete myelin internode segments along nearby axons. Oligodendrocytes have been studied intensively for decades, because of their important role in vertebrate evolution[1] and because their loss and failed regeneration contributes to debilitating diseases such as multiple sclerosis. However, much of our knowledge about the behavior of oligodendrocytes and the process of myelination comes from studies of developmental myelination in white matter[2]. These pioneering studies indicate that most oligodendrocytes are generated early in life, that myelination is a constitutive process primarily induced by the presence of an axon of appropriate diameter, and that myelination continues until the axon surface is covered (with the exception of gaps, the nodes of Ranvier, between myelin segments), leading to populations of myelinated and unmyelinated axons that are maintained throughout life[3].

Recent studies suggest that interactions between oligodendrocytes and neurons are far more complex and less static than previously envisioned. It is now clear that oligodendrocytes also provide crucial metabolic support to axons[4,5], which are often far removed from their cell bodies and have limited access to the extracellular environment. In addition, although oligodendrocyte generation (oligodendrogenesis) and myelination begin during the perinatal period[2], oligodendrocyte precursor cells (OPCs) persist throughout life and support de novo formation of oligodendrocytes in the adult CNS in the absence of demyelinating pathology[6–10]. Increasing neuronal activity has been shown to enhance the generation of oligodendrocytes and thickness of individual myelin segments[11], suggesting that the same changes in activity that induce synaptic plasticity and alter neuronal excitability can also modify myelination. Changes in myelination within white matter tracks have been associated with motor learning in humans[12,13], and recent studies in mice showed that blocking the formation of new oligodendrocytes impairs motor learning[14,15], suggesting that the generation of new myelin segments is an important form of plasticity used to modify the properties of circuits in the CNS.

However, our knowledge about this form of plasticity remains incomplete, in part because longitudinal studies of oligodendrocyte dynamics have not been performed in the intact CNS of adult mammals. Little is known about the extent to which oligodendrocytes and individual internode segments are remodeled in the adult brain or about what types of experiences induce these changes. This is particularly true for cortical circuits, where many axons exhibit discontinuous myelination[16], providing abundant territory for addition of new myelin and greater potential for remodeling of existing sheaths.

Here we performed longitudinal in vivo two-photon imaging in the somatosensory cortex of adult transgenic mice, in which oligodendrocytes and their individual myelin internodes can be resolved, to determine the extent of myelin dynamics in cortical gray matter. Our studies indicate that the period of oligodendrogenesis in the cerebral cortex is very prolonged, with more than half of oligodendrocytes in these circuits produced after four months of age. Although new oligodendrocytes were continually produced, their integration was highly inefficient, with a majority dying shortly after being generated. New myelin segments that appeared in the adult cortex were produced exclusively by newly generated

[1]The Solomon H. Snyder Department of Neuroscience, Johns Hopkins University School of Medicine, Baltimore, MD, USA. [2]Department of Cell and Developmental Biology, University of Colorado School of Medicine, Aurora, CO, USA. [3]Department of Neurology, Johns Hopkins University School of Medicine, Baltimore, MD, USA. [4]These authors contributed equally: Ethan G. Hughes and Jennifer L. Orthmann-Murphy. *e-mail: ethan.hughes@ucdenver.edu; dbergles@jhmi.edu

oligodendrocytes, rather than by formation of new internodes from existing cells. Long-term imaging of individual myelin sheaths revealed that the majority were extraordinarily stable, with only 1% changing in length over a period of seven weeks. Exposure of mice to sensory enrichment dramatically increased the frequency of new oligodendrocyte integration, but did not alter the rate of sheath remodeling. Together, these results indicate that changes in life experience in adulthood alter the pattern of myelination in the cerebral cortex primarily through production of new oligodendrocytes, thereby providing an additional substrate for circuit plasticity in the adult brain.

Results

Oligodendrocyte generation continues in the adult cortex. Previous assessments of myelination changes in mammals involving histological analysis[2], genetic fate tracing[6–10], and in vivo magnetic resonance imaging (for example, diffusion tensor imaging)[12,13] indicate that oligodendrogenesis and myelination also occurs in the adult CNS. Limitations of these approaches, particularly the restricted time and spatial resolution and the inability to assess cell turnover, can be overcome through longitudinal in vivo fluorescence microscopy, as shown by the powerful insight obtained into the process of developmental myelination in the spinal cords of zebrafish[17,18]. To determine the extent of myelination changes in adult mammalian cortex, we obtained BAC transgenic mice in which EGFP is expressed under control of the promoter/enhancer for myelin-associated oligodendrocyte basic protein (*Mobp-EGFP* mice; Gensat[19,20]), a major component of myelin sheaths that is expressed late in oligodendrocyte maturation[21]. Immunocytochemical analysis of the somatosensory cortex revealed that all EGFP$^+$ cells in this region co-localized with the oligodendrocyte protein 2′,3′-cyclic-nucleotide 3′-phosphodiesterase (CNPase), but not the OPC-associated protein NG2 (Supplementary Fig. 1a–c), and all CNPase immunoreactive (CNP$^+$) cells were also EGFP$^+$, indicating that this mouse line allows detection of the full complement of oligodendrocytes (Supplementary Fig. 1d). *Mobp-EGFP* mice also allowed unambiguous visualization of individual internode segments along axons, with paranodal regions, defined by contactin-associated protein 1 (Caspr) immunoreactivity and proximity to voltage gated sodium channels, exhibiting enhanced fluorescence (Fig. 1a–c), presumably due to EGFP accumulation in paranodal loops. Using a label-free imaging technique that visualizes compact myelin (spectral confocal reflectance microscopy, SCoRe)[22], we found that EGFP$^+$ internodes, but not paranodes, were detected with SCoRe (Fig. 1c), indicating that these EGFP$^+$ internodes represented cytoplasmic channels surrounding compact myelin. In humans, the molecular layer of the cortex (layer I) is enriched with tangentially oriented myelinated fibers that form the plexus of Exner[23]. In vivo two-photon imaging and volumetric analysis of the somatosensory cortex of *Mobp-EGFP* mice revealed that oligodendrocytes are similarly distributed throughout the upper layers of the murine cortex (Fig. 1d–g and Supplementary Video 1).

To assess what proportion of oligodendrocytes are added in adult life, we performed volumetric in vivo two-photon imaging in the somatosensory cortex of young adult (2–4 months), middle-aged (10–14 months), and aged (18–24 months) *Mobp-EGFP* mice. Although the relative distribution of oligodendrocytes in layers I–IV (0–400 µm) of somatosensory cortex remained similar across ages, more than half of the oligodendrocytes present in middle-aged mice were produced after 4 months of age (Fig. 1d–g). Oligodendrocyte density did not differ significantly between middle-aged and aged mice, indicating that oligodendrocytes reach their zenith by middle age (Fig. 1f). Although the density of oligodendrocytes varies by cortical depth (Fig. 1g), we found that integration of new oligodendrocytes was uniform across cortical layers I–IV of somatosensory cortex (Supplementary Fig. 2), whereas neuron density remained

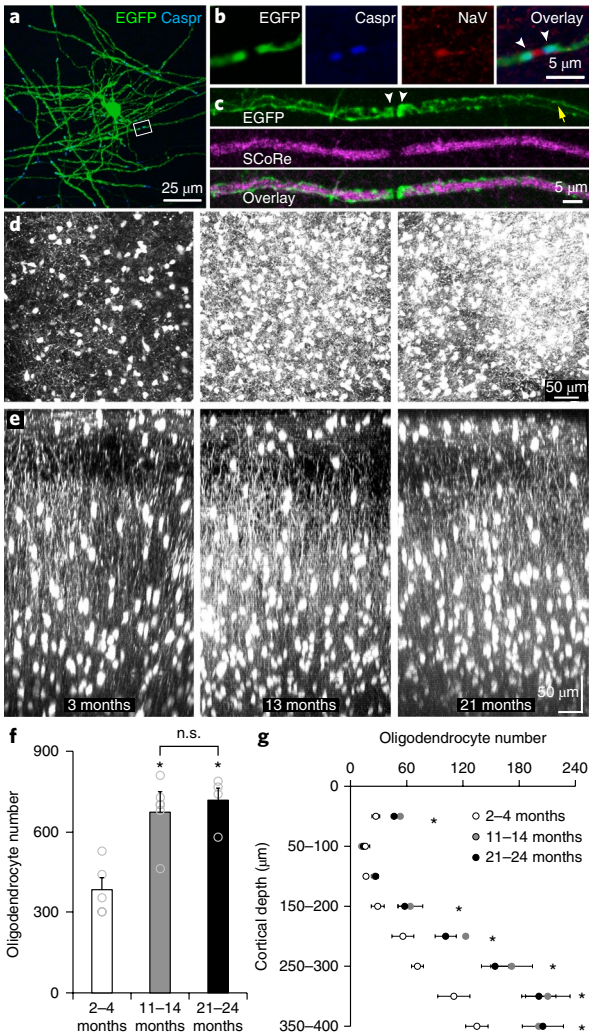

Fig. 1 | Oligodendrocyte density in upper cortical layers increases during adulthood. a, Maximum projection image of an example individual *Mobp-EGFP* oligodendrocyte from a horizontal section (0–50 µm from the pial surface, $n=5$ mice) immunolabeled with EGFP and Caspr. **b**, High-magnification area from **a**. Putative EGFP$^+$ paranodes (white arrowheads) are immunolabeled with Caspr and are adjacent to clustered voltage-gated sodium channels (NaV), indicating this is a node of Ranvier. **c**, Maximum projection of a putative EGFP$^+$ myelin sheath in a horizontal section (0–50 µm from the pial surface) immunolabeled with EGFP and imaged with SCoRe. Note the accumulation of EGFP within paranodes (white arrowheads) that lack SCoRe signal. EGFP is also present in cytoplasmic channels (yellow arrow) along the sheath, which has strong SCoRe signal indicative of compact myelin. **d**, Maximal *z*-projection of 400 µm of somatosensory cortex (postnatal day (P) 90, left; P395, middle; P630, right; $n=5$ *Mobp-EGFP* mice; chronic cranial window preparation; depth = 0–400 µm). **e**, Maximal *y*-projection of 200 µm of somatosensory cortex (P90, left; P395, middle; P630, right; *Mobp-EGFP* mice; chronic cranial window preparation). Note high density of oligodendrocytes in layer I. **f**, Quantification of oligodendrocyte number in layers I–IV (0–400 µm) of somatosensory cortex (425 µm × 425 µm × 400 µm; 2–4 months, $n=5$ mice; 11–14 months, $n=6$ mice; 21–24 months, $n=4$ mice; one-way ANOVA with Tukey post hoc test: 2–4 months vs. 11–14 months, $P=0.0001$, $q_{13}=9.14$; 2–4 months vs. 21–24 months, $P=0.0002$, $q_{13}=8.49$; 11–14 months vs. 21–24 months, $P=0.99$, $q_{13}=0.12$; n.s., not significant; $^*P<0.0005$). **g**, Quantification of total oligodendrocyte number in layers I–IV of somatosensory cortex (2–4 months, $n=5$ mice; 11–14 months, $n=6$ mice; 21–24 months, $n=4$ mice; $^*P<0.05$, one-way ANOVA with Tukey post hoc test). Data in **f**,**g** are presented as mean ± s.e.m.

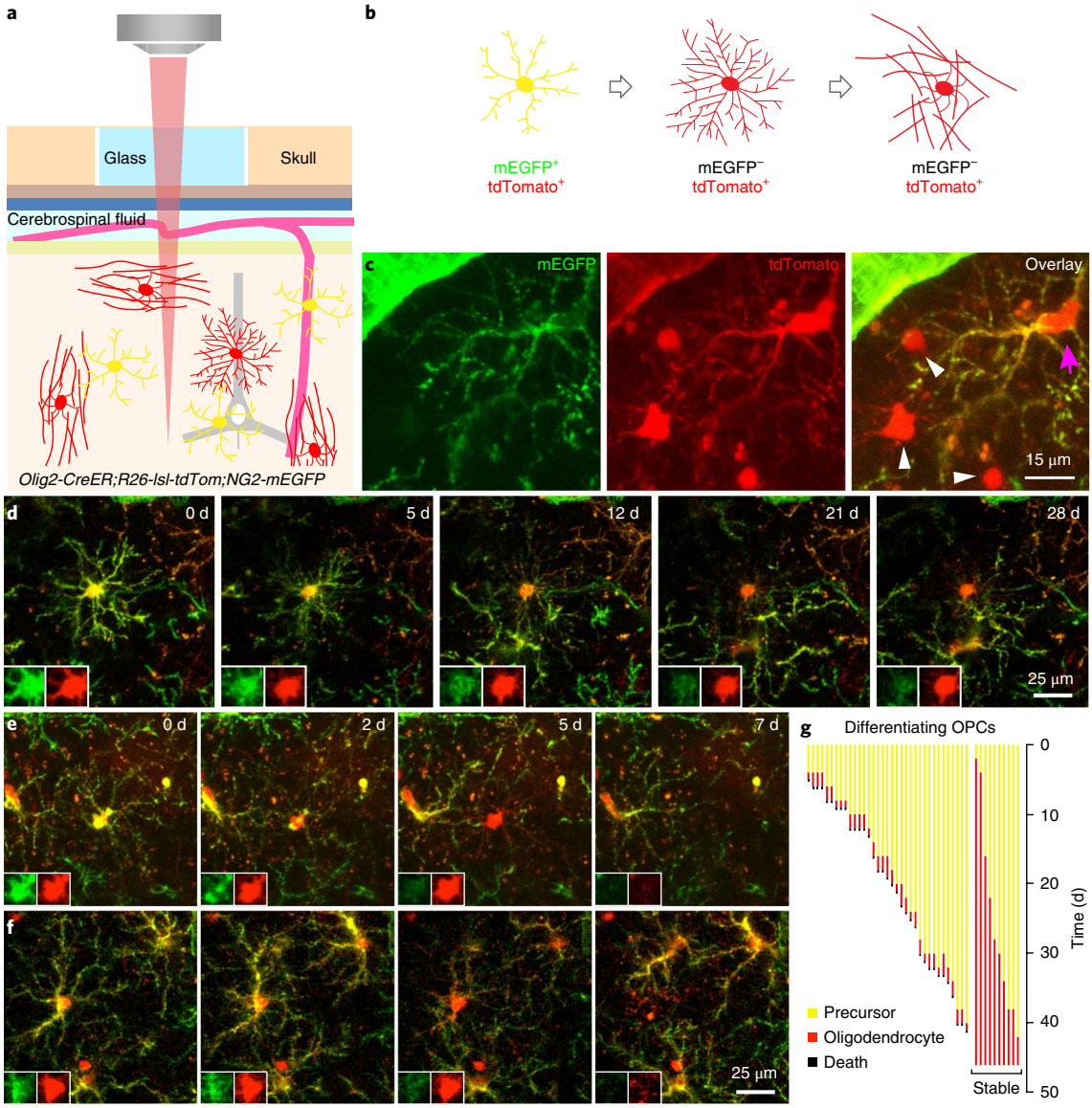

Fig. 2 | Inefficient integration of newly generated oligodendrocytes in the mature cortex. a, In vivo two-photon microscopy through chronic cranial windows in *Olig2-CreER;R26-lsl-tdTomato;NG2-mEGFP* triple transgenic mice. **b**, Membrane-anchored EGFP is expressed by OPCs, and all stages of the oligodendrocyte lineage (progenitors, premyelinating cells, and mature oligodendrocytes) express tdTomato following administration of tamoxifen. When OPCs differentiate, the NG2 promoter is downregulated and mEGFP is no longer expressed, while tdTomato is preserved. **c**, Maximal projection of mEGFP and tdTomato expression in a triple transgenic mouse (P150; depth = 10–19 μm; 100 mg/kg tamoxifen injected for 5 d at P30; $n = 5$ mice). OPCs (magenta arrow) express both fluorophores, but mature oligodendrocytes only express tdTomato (white arrowheads). Note pericyte expression of mEGFP. **d**, Maximal intensity projection images of a differentiating OPC that becomes a stably integrated oligodendrocyte (P240; depth = 111–120 μm). Images were acquired every 2–3 d for 28 d, and relative date of collection is shown on each panel. Insets show the cell soma at higher magnification for each fluorescent channel. **e**,**f**, Maximal intensity projection images of differentiating OPCs located 234–252 μm (**e**) and 27–61 μm (**f**) below the pial surface (P240). Images were acquired every 2–3 d for 1 week. Note the fragmentation of the cell at the 7-d timepoint in **f**. **g**, Quantification of maturation of differentiating OPCs over 1.5 months in P240–P426 mice ($n = 3$ mice, two imaging volumes per animal; mature oligodendrocytes = 10 of 45).

constant over the 24 months examined (Supplementary Fig. 3). The density of OPCs also remained unchanged over this time period (Supplementary Fig. 3f), in accordance with the homeostatic behavior of these precursors[24]. The prolonged period of oligodendrogenesis in the murine cortex has important implications for studies of circuit plasticity and remyelination, as such studies are often performed during a period of intense myelination (2–4 months of age)[11,14,15,25,26].

Most oligodendrocytes generated in the adult brain fail to integrate. During perinatal development, 20–50% of newly formed oligodendrocytes undergo programmed cell death following differentiation[27,28]; however, the rate of successful integration of oligodendrocytes in the adult CNS has not been determined. To follow the differentiation of OPCs into mature oligodendrocytes in vivo, we generated triple transgenic mice (*Olig2-CreER;R26-lsl-tdTomato;NG2-mEGFP*) in which the entire oligodendrocyte lineage expressed tdTomato, but mEGFP (membrane-anchored EGFP) was expressed only in OPCs (Fig. 2a–c and Supplementary Fig. 4). NG2 expression is rapidly downregulated when OPCs transform into oligodendrocytes, resulting in a loss of EGFP fluorescence[24], allowing us to monitor the generation and survival of newly generated

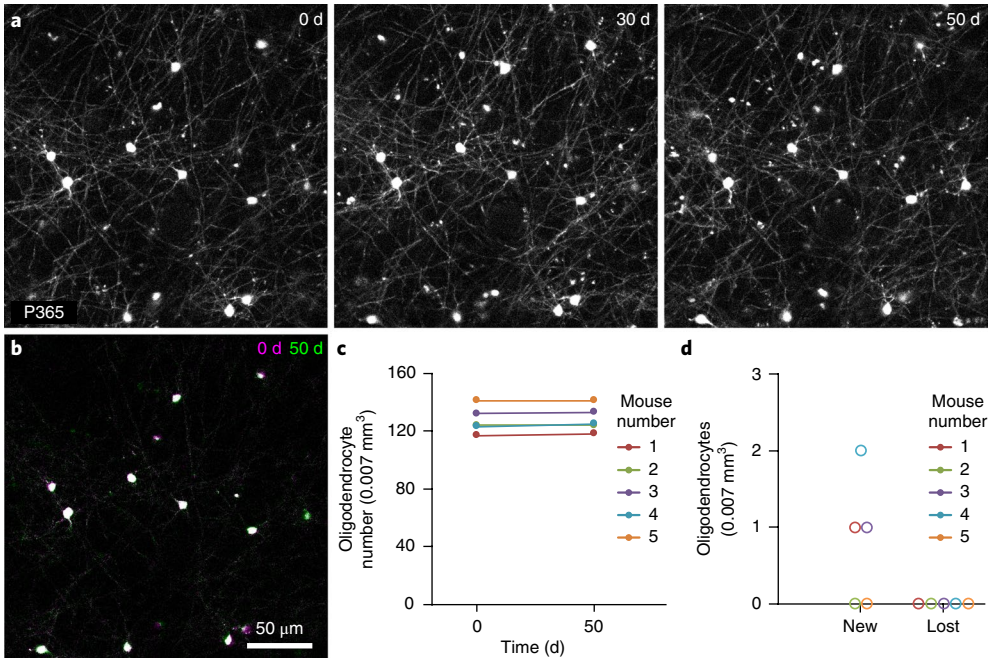

Fig. 3 | Oligodendrocytes are highly stable in the adult cortex. a, Maximal intensity projection images of oligodendrocytes in the somatosensory cortex of a *Mobp-EGFP* mouse (P365; depth = 45–50 µm). Images were acquired weekly for 50 d. **b**, Montage of 0 d (magenta) and 50 d (green) timepoints. Oligodendrocyte cell body position remains unchanged. **c**, Quantification of oligodendrocyte number over 50 d in >P365 mice. ($n = 5$ mice; cells = 641). **d**, Quantification of new or lost oligodendrocytes over 50 d in >P365 mice ($n = 5$ mice).

oligodendrocytes by imaging these two fluorophores. In middle-aged mice (8–14 months of age), OPCs (mEGFP$^+$tdTomato$^+$) extended dynamic, radially oriented processes that were studded with motile filopodia (Supplementary Videos 2 and 3). Upon differentiation, OPCs halted their migration and filopodial extension and instead extended long, fine processes characteristic of premyelinating oligodendrocytes (Fig. 2a–c and Supplementary Videos 2 and 3). This morphological change was accompanied by a decrease in EGFP fluorescence and invasion of processes from neighboring OPCs into the territory of the differentiating cell, consistent with downregulation of repulsive cues[24] (Fig. 2d–f). Oligodendrocytes that successfully integrated into the cortex remained tdTomato$^+$ throughout the duration of imaging (up to 40 d; Fig. 2d and Supplementary Video 2). However, many differentiating OPCs that lost EGFP fluorescence and displayed premyelinating oligodendrocyte morphology were present only transiently; within 1.8 ± 0.1 d of reducing mEGFP expression, they abruptly disappeared (35 cells; $n = 3$ mice, 8–14 months old). In rare cases, fragmentation of these cells was observed (Fig. 2f and Supplementary Video 3), suggesting that they underwent programmed cell death. The death of newly formed oligodendrocytes was a rare event in the middle-aged cortex, occurring at a rate of 0.22 ± 0.08 events per day ($n = 3$ mice, 8–14 months old, imaged over 1.5 months), but the majority of OPCs that differentiated in the middle-aged cortex died at the premyelinating stage, with only 22% becoming stably integrated into these circuits (10 of 45 differentiating oligodendrocytes, $n = 3$ mice, 8–14 months old; Fig. 2g). The death of premyelinating oligodendrocytes was distinct from the occasional turnover of OPCs, which was characterized by retraction of their processes and retention of both mEGFP and tdTomato until the cell disappeared (Supplementary Fig. 5). Although we were unable to track cells beyond about 2 months because of skull regrowth, the lack of oligodendrocyte death in *Mobp-EGFP* mice suggests that this minority of cells becomes stably integrated. To determine whether in vivo imaging may have decreased the viability of newly formed oligodendrocytes, we examined the proliferation of OPCs in longitudinally imaged *Olig2-CreER;R26-lsl-tdTomato;NG2-mEGFP* mice. OPCs homeostatically maintain their density[24], so phototoxicity-induced death of newly formed oligodendrocytes would be expected to enhance OPC proliferation. We found that OPC proliferation averaged 0.74 ± 0.09 events per day in *Olig2-CreER;R26-lsl-tdTomato;NG2-mEGFP* mice ($n = 3$ mice, 8–14 months old, tracked cells = 478) compared to 1.5 ± 0.1 events per day in *NG2-mEGFP* mice ($n = 5$ mice, 3–5 months old, tracked cells = 1,118)[24], suggesting that the infrequent integration of newly formed oligodendrocytes does not reflect their increased sensitivity to longitudinal in vivo imaging.

Oligodendrogenesis supplements existing myelin in the mature brain. Previous studies have shown that some oligodendrocytes undergo apoptosis in the adult brain[29], suggesting that oligodendrogenesis may not just supplement existing myelin, but also replace oligodendrocytes lost through normal aging[9]. This scenario is attractive, as it provides an explanation for the persistence of OPCs throughout the CNS, where they remain abundant and widely distributed. However, ^{14}C birthdating and recent genetic fate-mapping approaches suggest that most oligodendrocytes in the human brain have long lifespans[7,30]. To determine whether oligodendrogenesis in the adult somatosensory cortex contributes to homeostatic maintenance of the oligodendrocyte population, we used in vivo two-photon imaging to track individual oligodendrocytes in the cortex of middle-aged mice. Notably, every one of the approximately 600 oligodendrocytes monitored over this period was stable for >1.7 months (Fig. 3). A small number of new oligodendrocytes were generated over this time period, adding to the total population. These results indicate that there is minimal turnover of oligodendrocytes in the normal adult cortex and that oligodendrogenesis continually expands the population of myelinating cells.

Discontinuous myelination persists in the adult brain. A recent study using serial electron microscopic reconstruction from an

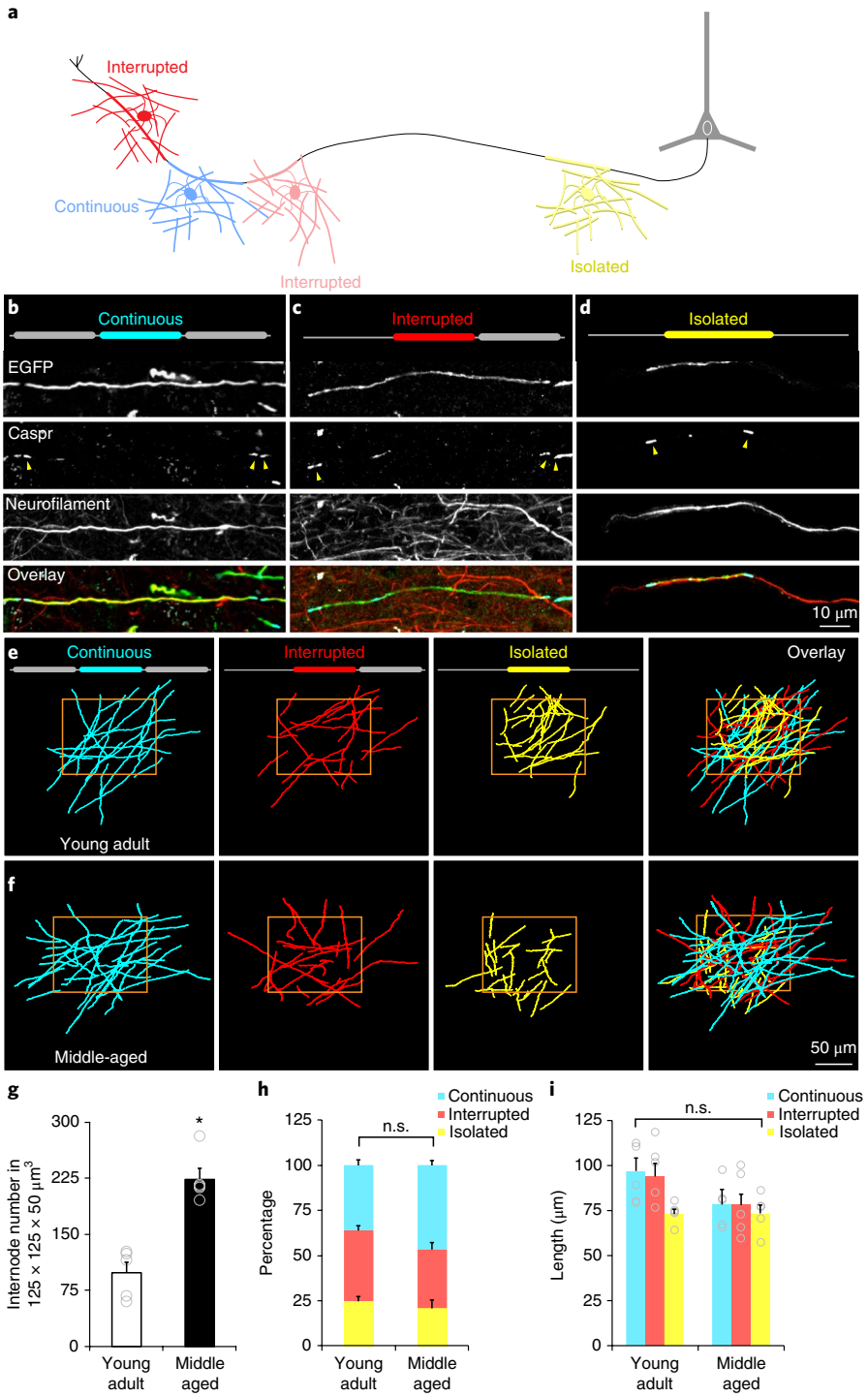

Fig. 4 | Discontinuous myelination persists in the adult brain. a, Schematic of myelin sheath categorization by the presence or absence of neighboring sheaths. **b**, Maximum projection of a continuous myelin sheath. Note doublets of Caspr immunolabeling at both ends of the sheath (yellow arrowheads). **c**, Maximum projection of an interrupted myelin sheath. Note a doublet of Caspr immunolabeling at one end of the sheath (yellow arrowheads) and the axon extending beyond the Caspr singlet. **d**, Maximum projection of an isolated myelin sheath. Note that only singlets of Caspr immunolabeling appear at the ends of the sheath (yellow arrowheads) and that the axon extends beyond ends of the sheath. **e**, Projection of traces of EGFP$^+$ myelin internodes within a $125 \times 125 \times 50\ \mu m^3$ volume in the somatosensory cortex of a *Mobp-EGFP* mouse (P90; depth = 0–50 µm; $n = 5$ mice). Positions of neighboring internodes on the same axon were used to characterize internodes as continuous, interrupted, or isolated (configuration illustrated by diagram at top of each panel). **f**, Projection of traces of EGFP$^+$ myelin internodes within $125\ \mu m^2$ area in the somatosensory cortex of a *Mobp-EGFP* mouse (P365; depth = 0–50 µm). **g–i**, Quantification of the (**g**) number (young adult: $n = 5$ mice; middle-aged: $n = 5$ mice, $^*P > 0.0005$, $t_8 = -6.02$, two-tailed Student's t test), (**h**) proportion (young adult: $n = 5$ mice; middle-aged: $n = 5$ mice; continuous, $P = 0.17$, $t_8 = -1.52$; interrupted, $P = 0.08$, $t_8 = 1.98$; isolated, $P = 0.53$, $t_8 = 0.65$, two-tailed Student's t test), and (**i**) length of each internode class (young adult: $n = 5$ mice; middle-aged: $n = 5$ mice; continuous, $P = 0.13$, $t_8 = -1.68$; interrupted, $P = 0.12$, $t_8 = -1.72$; isolated, $P = 0.97$, $t_8 = -0.04$, two-tailed Student's t test) within a $125 \times 125 \times 50\ \mu m^3$ volume, for oligodendrocytes within layer I of somatosensory cortex. Data are presented as mean ± s.e.m.; n.s., not significant.

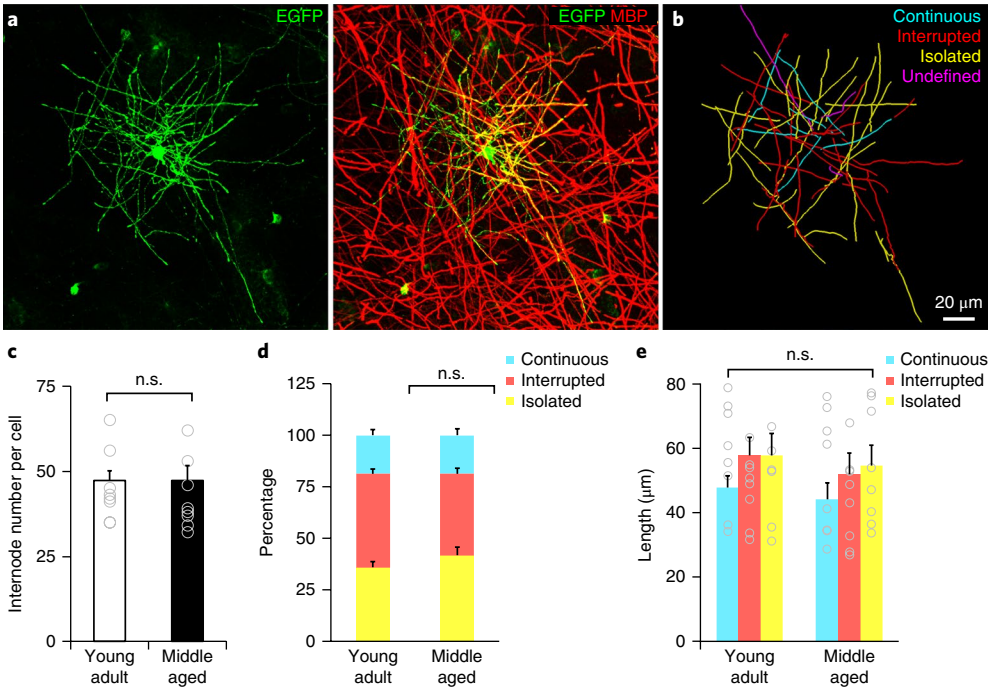

Fig. 5 | Individual oligodendrocytes generate both continuous and isolated internodes. a, Maximum projection of an oligodendrocyte (P90; depth = 50–100 µm) labeled with AAV9-MBP-EGFP (left) and immunostained with an antibody against MBP (right). **b**, Traces of EGFP$^+$ myelin internodes of the oligodendrocyte shown in **a**. Each internode was classified as continuous, interrupted, isolated, or undefined (projects out of tissue section). **c**–**e**, Quantification of (**c**) number (young adult: $n = 5$ mice, 8 cells; middle-aged: $n = 5$ mice, 8 cells; $P = 0.62$, $t_{14} = 0.51$, two-tailed Student's t test), (**d**) proportion (young adult: $n = 5$ mice, 8 cells; middle-aged: $n = 5$ mice, 8 cells; continuous, $P = 0.99$, $t_{14} = -0.005$; interrupted, $P = 0.11$, $t_{14} = 1.70$; isolated, $P = 0.27$, $t_{14} = -1.15$, two-tailed Student's t test), and (**e**) length of each internode class (young adult: $n = 5$ mice, 8 cells; middle-aged: $n = 5$ mice, 8 cells; continuous, $P = 0.59$, $t_{14} = 0.55$; interrupted, $P = 0.52$, $t_{14} = 0.65$; isolated, $P = 0.73$, $t_{14} = 0.36$, two-tailed Student's t test; n.s., not significant) for individual oligodendrocytes within layer I of cortex. Data are presented as mean ± s.e.m.

adult mouse (3–4 months) reported that many axons in layer II/III of the visual cortex exhibit discontinuous myelination, in which segments of myelin were often bordered by long stretches of axon devoid of myelin[16]. To determine whether this phenomenon reflects an extended time-course of myelination in the cortex (Fig. 1) or a stable pattern of partial myelination, we compared the distribution of myelin internodes of layer I oligodendrocytes between young adult and middle-aged *Mobp-EGFP* mice. We classified all myelin sheaths in a $125 \times 125 \times 50\ \mu m^3$ volume into three categories: continuous, interrupted, or isolated. If the ends of the sheath were bordered by nodes of Ranvier on either side (abutting two other internodes), a sheath was classified as continuous; if one side bordered a node of Ranvier and the other a bare segment of axon, it was classified as interrupted; and if an internode was bordered by bare axon on either side, it was classified as isolated (Fig. 4a–d). Isolated sheaths did not reflect short axons with only one myelin sheath, as they were found on axons that extended substantial distances within the imaging field (Fig. 4d). In both young and middle age mice, internodes in each of these categories were present in the somatosensory cortex (Fig. 4e,f), indicating that discontinuous myelination is not simply a feature of prolonged myelination. Despite the robust increase in density of myelin sheaths over this time period (Fig. 4g), the relative proportions of internodes in each category were similar, although there was a trend toward more continuous internodes in middle-aged mice (36% versus 47%, young adult: $n = 5$ mice; middle-aged: $n = 5$ mice, $P = 0.17$, $t_8 = -1.52$, two-tailed Student's t test; Fig. 4h). Moreover, the lengths of internodes, independent of category, were stable during this time (Fig. 4i). These results suggest that oligodendrocytes, once formed, establish defined domains along axons that do not require interactions with other myelin segments for stability.

Since the initial description oligodendrocytes, it has been postulated that there is heterogeneity within this glial cell type[31], a conclusion supported by recent single-cell RNA-seq analysis[32] and the existence of a subpopulation of cortical oligodendrocytes with short, numerous myelin sheaths[33]. To determine whether oligodendrocytes vary in their production of different types of myelin sheaths (continuous, interrupted, or isolated), we labeled individual oligodendrocytes using an adeno-associated virus expressing EGFP under the control of a fragment of the myelin basic protein (MBP) promoter (Fig. 5a,b). We found that oligodendrocytes in both young and middle-aged animals produced a similar number of myelin sheaths (Fig. 5c; young adult: 45 ± 4 sheaths, $n = 5$ mice, 8 cells; middle-aged: 43 ± 4 sheaths, $n = 5$ mice, 8 cells; $P = 0.62$, $t_{14} = 0.51$, two-tailed Student's t test) and equivalent proportions of continuous, interrupted, and isolated sheaths (Fig. 5d; young adult: $n = 5$ mice, 8 cells; middle-aged: $n = 5$ mice, 8 cells; continuous, $P = 0.99$, $t_{14} = -0.005$; interrupted, $P = 0.11$, $t_{14} = 1.70$; isolated, $P = 0.27$, $t_{14} = -1.15$, two-tailed Student's t test). Moreover, myelin sheaths of oligodendrocytes in young and middle-aged animals were of similar lengths (Fig. 5e; young adult: $n = 5$ mice, 8 cells; middle-aged: $n = 5$ mice, 8 cells; continuous, $P = 0.59$, $t_{14} = 0.55$; interrupted, $P = 0.52$, $t_{14} = 0.65$; isolated, $P = 0.73$, $t_{14} = 0.36$, two-tailed Student's t test). These results indicate that oligodendrocytes adopt similar morphologies in the adult brain, despite being separated in generational time by ~8 months, suggesting that the constraints that limit target selection and internode length are conserved over this extended period of life.

Internode remodeling in the adult brain. Developmental studies indicate that the arrangement of internodes formed by each

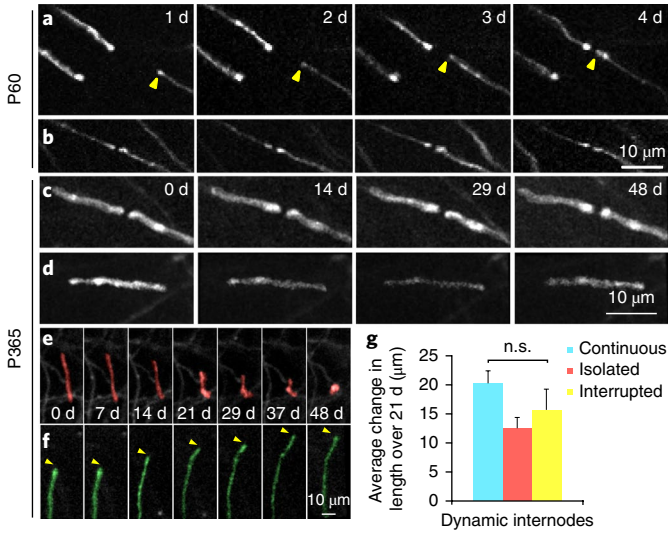

Fig. 6 | Infrequent remodeling of myelin internodes in the somatosensory cortex. a, In vivo time-lapse images of oligodendrocyte processes in *Mobp-EGFP* mice ($n=5$ mice). An extending process of a newly generated oligodendrocyte (yellow arrowhead) that forms a new node of Ranvier. **b**, An existing node exhibits little change in structure over 4 d (P60; depth = 24–27 µm; thinned-skull preparation, $n=5$ mice). **c**,**d**, Maximal intensity projection image of (**c**) continuous internodes (P365; depth = 39–43 µm) and (**d**) an isolated internode (P365; depth = 31–35 µm) that remain unchanged over 48 d. **e**, Maximal intensity projection images illustrating retraction of an internode (red; P365; depth = 63–67 µm). **f**, Maximal intensity projection image illustrating extension of an internode (green; P365; depth = 63–67 µm). No newly generated or dying oligodendrocytes were found within 250 µm of these internodes. **g**, Quantification of the average change in length of dynamic internodes over 3 weeks in P365 mice. ($n=20$ mice, $P=0.62$, $F_{3,35}=0.49$, one-way ANOVA; n.s., not significant; mean ± s.e.m.).

oligodendrocyte is established within a restricted time-window after oligodendrocyte specification[34,35]. Although myelin sheath lengths decrease with aging[36,37] and adult-born oligodendrocytes have been shown to form shorter myelin sheaths[9], it is not known whether oligodendrocytes have the capacity to remodel the length or position of internodes after this critical period. Such rearrangements would allow matching of sheath characteristics to changes in axon properties, such as rates of activity[17,18]. To determine whether the lengths of existing myelin sheaths are altered in cortical circuits, we monitored individual myelin sheaths and nodes of Ranvier in the somatosensory cortex of young adult and middle-aged *Mobp-EGFP* mice in vivo. Stable integration of a new oligodendrocyte resulted in the concomitant appearance of new myelin sheaths in the vicinity of the cell body that gradually increased in length before stabilizing, often concluding with the formation of nodes of Ranvier (Fig. 6a and Supplementary Video 4). In accordance with our internode analysis (Fig. 4), oligodendrocytes also formed myelin segments along axons that were previously unmyelinated or sparsely myelinated, and these sheaths remained isolated for the duration of the imaging period (up to 3 weeks; Supplementary Fig. 6). Thus, isolated internodes were not the net result of stranding, due to gradual removal of surrounding internodes, but rather the result of formation of new myelin sheaths along portions of axons that were previously devoid of myelin.

To define the extent of morphological reorganization of myelin sheaths in the middle-aged somatosensory cortex, we repeatedly imaged individual sheaths for 50 days. The majority of existing myelin sheaths and nodes of Ranvier remained constant in length and position throughout this time (Fig. 6b–d). However, a small fraction of myelin sheaths underwent retraction or extension (percentage of dynamic internodes: 0.97 ± 0.5%, $n=5$ mice, 10–14 months old; Fig. 6e,f and Supplementary Videos 5 and 6). Although it might be expected that isolated sheaths have greater opportunity for length changes, dynamic myelin sheaths were equally represented across continuous, interrupted, and isolated categories, and the average change in length (~15 µm) did not differ across these classifications (Fig. 6g; $P=0.58$, one-way ANOVA). Hypertrophic EGFP$^+$CNP$^+$ processes that lacked MBP immunoreactivity (Supplementary Fig. 7), a morphology similar to the retracting sheaths detected through in vivo imaging, were also observed in *Mobp-EGFP* mice not subjected to cranial window surgery, suggesting that such events were not solely the result of experimental procedures associated with in vivo imaging. Together, these data indicate that the position and length of individual myelin sheaths are remarkably stable within cortical circuits.

Sensory enrichment enhances oligodendrogenesis and myelination in the adult brain. Studies in the developing prefrontal cortex have shown that social isolation leads to profound decreases in sheath number, sheath thickness, and myelin protein expression[25,26], indicating that changes in myelination can be induced independent of oligodendrogenesis. However, the extent to which different features of myelin are influenced by life experience in the adult cortex remains poorly understood. To determine whether myelin sheath length remodeling is influenced by sensory experience in the somatosensory cortex, we monitored internode dynamics in middle-aged *Mobp-EGFP* mice that experienced enhanced sensory input, induced by housing mice in cages fitted with hanging strings of beads (Fig. 7a). Subjecting mice to this novel sensory experience has been shown to increase dendritic spine formation in the upper layers of somatosensory (barrel) cortex and promote long-lasting memory formation[38]. Repetitive time-lapse imaging of internodes in this region revealed that exposure to this enhanced sensory experience did not alter the rate of extension or retraction of myelin sheaths, nor did it influence the proportion of sheaths that were dynamic compared to control animals (Fig. 7). Thus, although changes in the length of individual sheaths occur at a low rate in the somatosensory cortex of naive mice, this form of myelin reorganization is not strongly influenced by sensory experience.

Previous studies have shown that oligodendrogenesis can be increased in young adult animals (<1–3 months) by experimentally increasing neuronal activity or by altering social experience[11,25,26]. To determine whether changes in sensory experience modulate oligodendrogenesis in the middle-aged brain after the majority of myelination is complete, we compared new oligodendrocyte formation in the barrel cortex of *Mobp-EGFP* mice (10–14 months) housed in standard or sensory enriched cages (Fig. 7a). Sensory enrichment over a period of 20–22 days resulted in a fivefold increase in successfully integrated oligodendrocytes (primarily in layers II/III; Fig. 8), expanding the total oligodendrocyte population by 1.1 ± 0.2% and resulting in the addition of approximately 250 new myelin sheaths (assuming that each oligodendrocyte generates approximately 50 myelin sheaths[39]; Fig. 5c). This increase in myelin required whisker stimulation, as mice that had had their whiskers trimmed but were housed in the same sensory-enriched environment did not exhibit increases in oligodendrogenesis (Fig. 8c,d). Oligodendrocytes generated as a result of sensory enrichment remained in the cortex for an additional 3 weeks after the mice were returned to standard housing conditions (Supplementary Fig. 8), indicating that these cells became stably integrated into cortical circuits. Together, these data reveal that sensory experience in adult life modifies the pattern of myelination in the somatosensory cortex by altering the production of oligodendrocytes.

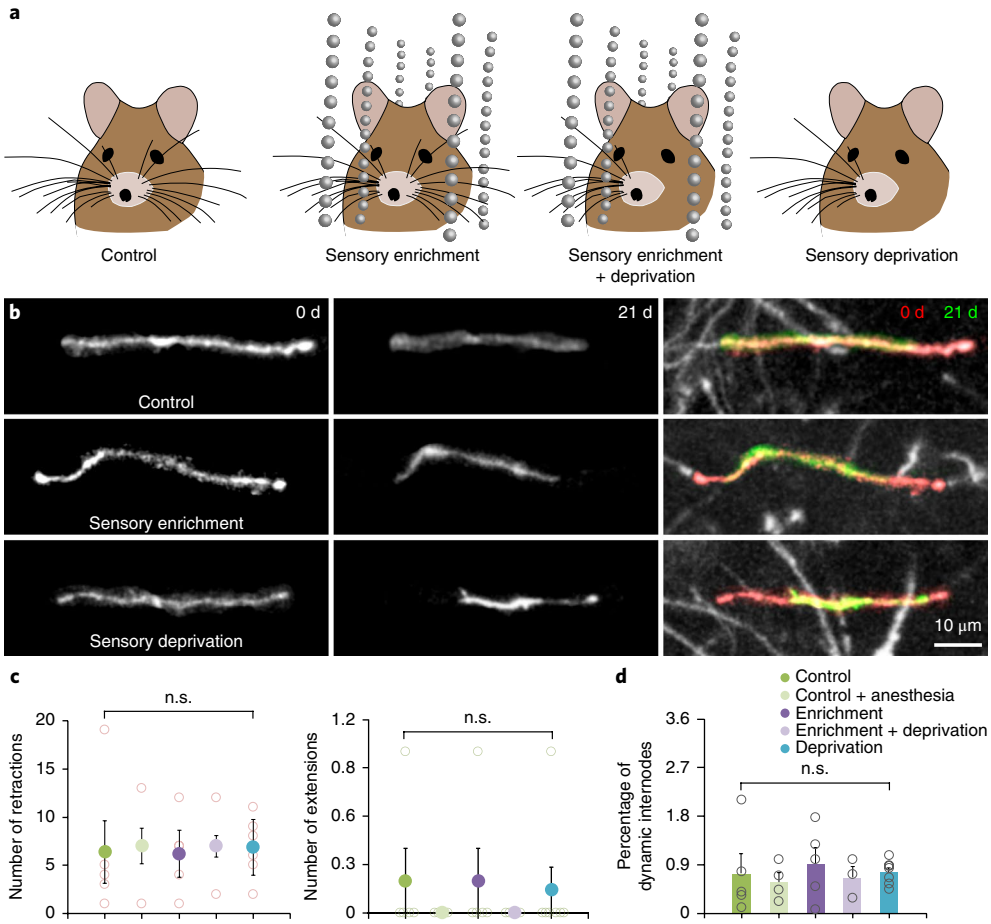

Fig. 7 | Sensory enrichment does not influence myelin remodeling in middle-aged animals. a, Illustration of different configurations to test role of sensory enrichment on myelin dynamics. Mice are housed in cages with or without sensory enrichment (hanging beads), or with left-side whiskers removed (deprivation) or not removed, for 21 d. **b**, Maximal intensity projection images of internodes imaged in the right somatosensory barrel cortex (top, P365; depth = 150–159 µm; middle, P365; depth = 183–192 µm; bottom, P365; depth = 210–232 µm) that decrease in length over 21 d. Red areas in overlay highlight extent of retraction. **c**, Quantification of internode retraction (left) and extension (right) over 21 d in P365 mice in a 425 × 425 × 100 µm^3 volume. Individual mouse values, open circles; mean value, filled circles (control, $n = 6$ mice; control + anesthesia, $n = 4$ mice; enrichment, $n = 5$; enrichment + deprivation, $n = 3$ mice; deprivation, $n = 7$ mice; retractions, $P = 0.99$, $F_{4,19} = 0.03$; extensions, $P = 0.86$, $F_{4,19} = 0.32$; one-way ANOVA). **d**, Quantification of percentage of total internodes that were dynamic over 21 d in P365 mice in a 425 × 425 × 100 µm^3 volume. Individual mouse values, open circles; mean value, filled circles (control, $n = 6$ mice; control + anesthesia, $n = 4$ mice; enrichment, $n = 5$; enrichment + deprivation, $n = 3$ mice; deprivation, $n = 7$ mice; $P = 0.91$, $F_{4,19} = 0.25$, one-way ANOVA; n.s., not significant). Data in **c**,**d** are presented as mean ± s.e.m.

Discussion

The cerebral cortex plays a crucial role in processing sensory information and enabling higher cognitive ability. Although classically defined as a gray matter region, some axons that reside in the cortex become ensheathed with myelin, a phenomenon that coincides with the maturation of functional properties[2]. However, even in the adult brain, many axons in the cortex remain unmyelinated or partially myelinated[16], providing abundant territory for the formation of new myelin sheaths. Recent studies indicate that oligodendrocytes continue to be generated in the cortex into adulthood[2,6–10] and that key features of myelin, including the thickness and length of sheaths, can be modified by neuronal activity[11,25,26], suggesting that formation of new myelin sheaths and remodeling of existing sheaths may represent additional forms of activity-dependent plasticity used to adapt the properties of cortical circuits to life experience. However, much of our knowledge about myelin plasticity comes from studies in white matter and early stages of life or has been inferred from indirect measures of myelination. Much less is known about the dynamics of oligodendrocytes and myelin sheaths in mature cortical circuits under physiological conditions.

Our studies indicate that oligodendrocyte formation continues over a very extended time-course in the cortex, with oligodendrocytes doubling in number from 4 to 10 months of age. The generation of oligodendrocytes was highly inefficient, with less than one-quarter of differentiation events leading to stable integration. However, oligodendrocytes that became integrated were remarkably stable, with no turnover observed over a period of almost 2 months. Although there are many potential means of modifying myelin, few sheaths changed their lengths or were removed over this period, and the degree of remodeling that was observed was not modified by sensory experience. In contrast, oligodendrogenesis was profoundly increased when animals were exposed to enhanced sensory experience, resulting in the formation of hundreds of new myelin sheaths in barrel cortex. This ability to change the pattern of myelination in the somatosensory cortex by producing new oligodendrocytes provides an additional substrate for modifying the processing capabilities of mature cortical circuits in response to life experience.

The process of developmental myelination in the CNS is inefficient, characterized by apoptotic death of many oligodendrocytes during the premyelinating stage[27,28], suggesting that there is a critical

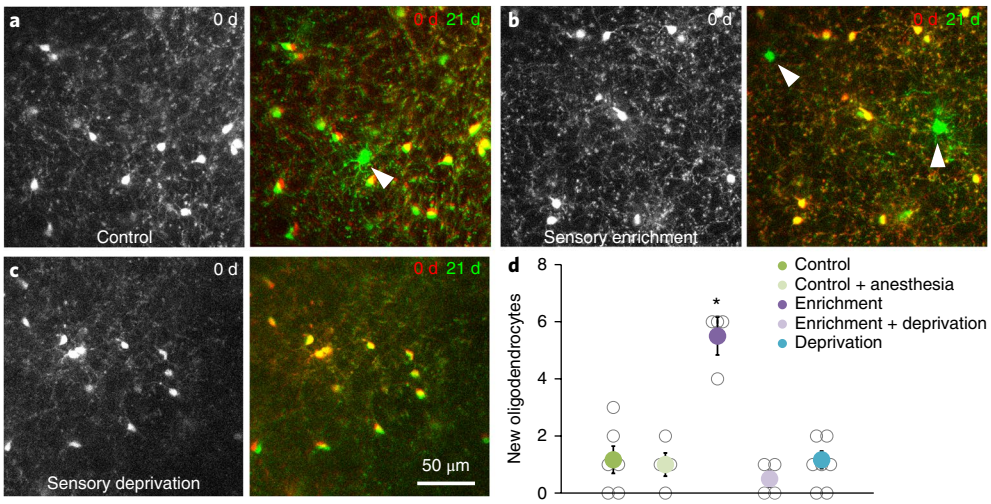

Fig. 8 | Sensory enrichment increases oligodendrogenesis in middle-aged animals. a–c, In vivo imaging of oligodendrocytes in the somatosensory cortex of *Mobp-EGFP* mice (P365; depth = 300–312 µm) showing the density of oligodendrocytes in one imaging field on day 0 (left) and an overlay of the same field on day 0 and day 21 (right). Control mouse in standard housing (**a**), mouse housed with sensory enrichment (**b**), and mouse in standard housing without whiskers (**c**). New oligodendrocytes are marked with white arrowheads. **d**, Quantification of oligodendrocyte addition over 3 weeks in P365 mice in a 425 × 425 × 400 µm^3 volume (control, $n = 6$ mice; control + anesthesia, $n = 4$ mice; enrichment, $n = 4$; enrichment + deprivation, $n = 4$ mice; deprivation, $n = 7$ mice; $^*P < 0.001$, one-way ANOVA with Tukey's post hoc test; mean ± s.e.m.).

time-window for integration and that the threshold for integration is high. Our studies indicate that although OPCs continue to differentiate in the adult brain, the barriers to full maturation and integration in these mature circuits remain high, with only a small fraction of these differentiation events leading to the formation of new myelin sheaths (Fig. 2). This inefficient process can be tolerated without jeopardizing future myelination, because it does not ultimately deplete the brain of progenitors[24]. Recent studies indicate that interneurons in the spinal cord prevent their myelination through expression of junctional adhesion molecule 2 (JAM2)[40]. Although there are likely many factors influencing oligodendrocyte survival, the expression of similar inhibitory cues by cortical axons could restrict the ability of nascent sheaths to proceed past developmental checkpoints within a critical time-window after differentiation has been initiated.

Once differentiating OPCs were successfully integrated as oligodendrocytes, they were highly stable in the adult cortex. We did not observe loss of a single oligodendrocyte using longitudinal in vivo imaging in middle-aged mice over 50 days of observation (Fig. 3), and adult-born oligodendrocytes that became stably integrated were observed up to 40 days following initial integration (Fig. 2g and Supplementary Fig. 8b). These data are consistent with recent findings using ^{14}C dating in humans showing that oligodendrocytes are largely stable throughout life[7] and with a genetic fate-mapping study in mice that suggests that adult-born oligodendrocytes in the murine brain have a half-life of over 10 years[30].

Living imaging studies in developing zebrafish have shown that new oligodendrocytes generate their myelin sheaths within 5 h and remain stable for 2–3 weeks[34]. However, whether existing myelin sheaths of mature oligodendrocytes retain the capacity for remodeling remains unclear. Young et al. reported that adult-born oligodendrocytes in the completely myelinated optic nerve produce more numerous and shorter internodes than oligodendrocytes formed during early development[9], suggesting that pre-existing myelin can be remodeled to accommodate newly formed myelin sheaths. Our in vivo longitudinal studies of individual myelin sheaths in the adult somatosensory cortex indicated that existing myelin sheaths rarely changed their length (Fig. 6), perhaps because of the extensive unmyelinated regions available.

Our distribution analysis of individual myelin sheaths in the middle-aged brain indicated that discontinuous myelination was sustained in animals up to 1 year of age (Fig. 4), indicating that it did not reflect an early developmental process. Reconstruction of individual oligodendrocytes revealed that each provided sheaths that could be isolated or could form part of a larger myelinated segment made up of multiple internodes, suggesting that these sheaths did not arise from cell autonomous differences among oligodendrocytes (Fig. 5). Time-lapse imaging further revealed that newly generated oligodendrocytes formed isolated sheaths on previously unmyelinated axons (Supplementary Fig. 6), indicating that these sheaths did not become isolated through removal or retraction of neighboring sheaths, although sheath retraction was occasionally observed (Fig. 6).

The function of discontinuous myelination in the cortex remains uncertain. Isolated sheaths may still enable oligodendrocytes to provide metabolic support to axons[4,5], although the ability of surrounding unmyelinated regions to access the extracellular environment would seem to reduce the necessity of transferring energy substrates such as lactate from oligodendrocytes. Subtle differences in action potential conduction and membrane excitability induced by these sheaths may create sufficient timing differences to alter the processing of information in cortical circuits. Future studies in which myelination can be selectively disrupted within defined circuits will help test these possibilities.

The doubling of oligodendrocyte number from young adulthood to middle age that we observed in the somatosensory cortex (Fig. 1) is consistent with results of ^{14}C dating in humans, which indicate that the number of oligodendrocytes in the cortex does not plateau until the fourth decade of life[7]. Many studies of cortical function and plasticity, as well as the recovery from demyelination, have been performed at an age when myelination patterns are immature, which may increase their ability to contribute to plasticity[14,15]. Our longitudinal studies of oligodendrogenesis and internode dynamics revealed that sensory enrichment enhanced myelination by stimulating the production of new oligodendrocytes, rather than by inducing the formation of new sheaths by existing oligodendrocytes (Fig. 8). The eventual reduction in ability to produce new oligodendrocytes in the aged brain, whether through a decrease in

suitable substrates (i.e., axons with a low threshold for myelination) or through aging-related decline in the ability of OPCs to undergo differentiation[41], may contribute to the decline in cognitive ability with age[37].

Our analysis of oligodendrocytes focused exclusively on layers I–IV due to limitations in the ability to resolve structures at great depth using two-photon EGFP imaging. It is possible that oligodendrocyte behavior may differ between gray and white matter regions in the adult CNS and/or between these regions and deeper layers of the cortex. Indeed, the kinetics of oligodendrocyte generation differs between gray and white matter[6–8], and it has been proposed that the prolonged period of oligodendrocyte generation and sparse myelination of the cortex may have a role in higher brain function[7]. Application of new approaches for deep-brain high-resolution imaging[42] of regions such as the corpus callosum will be necessary to define oligodendrocyte and myelin sheath dynamics in adult white matter.

Our data indicate that sensory experience modifies the integration of new oligodendrocytes, but does not induce existing oligodendrocytes to form new sheaths or alter the length of their sheaths (Figs. 7 and 8). However, it is possible that other structural and functional aspects of myelin not assessed here, such as sheath thickness[11,25,26] or metabolic support[4,5], could be modified in this context or that sheath remodeling occurs with a delay of many weeks after sensory enrichment. As we learn more about the identity of myelinated axons in the cerebral cortex[43], we will be able to assess how discrete patterns of activity influence the structure and stability of myelin, as well as the contributions of these changes to cortical function and behavior.

Analysis of demyelinated areas in brain tissue from human multiple sclerosis patients revealed a high incidence of oligodendrocytes with a premyelinating morphology[44], suggesting that the process of oligodendrocyte maturation may be stalled. Our time-lapse imaging of OPC maturation in the cortex (Fig. 2) indicated that this premyelinating stage was normally fleeting and that cells that did not integrate underwent apoptosis and were rapidly removed. Although the premyelinating stage may be stabilized in the lesion environment, it is also possible that the presence of premyelinating cells reflects continuous oligodendrogenesis due to failed integration. Identification of factors that promote this later stage of maturation, or that lower barriers to integration, may work synergistically with agents that promote the differentiation of OPCs[45] to further enhance remyelination and lesion repair and to promote functional recovery in disease and injury contexts.

Methods

Methods, including statements of data availability and any associated accession codes and references, are available at https://doi.org/10.1038/s41593-018-0121-5.

Received: 24 August 2017; Accepted: 9 February 2018;
Published online: 19 March 2018

References

1. Nave, K.-A. Myelination and support of axonal integrity by glia. *Nature* **468**, 244–252 (2010).
2. Yakovlev, P. I. & Lecours, A. R. The myelogenetic cycles of regional maturation of the brain. In: A. Minkowski ed. *Regional Development of the Brain in Early Life* 3–70 (Blackwell Scientific, Oxford, 1967).
3. Baumann, N. & Pham-Dinh, D. Biology of oligodendrocyte and myelin in the mammalian central nervous system. *Physiol. Rev.* **81**, 871–927 (2001).
4. Fünfschilling, U. et al. Glycolytic oligodendrocytes maintain myelin and long-term axonal integrity. *Nature* **485**, 517–521 (2012).
5. Lee, Y. et al. Oligodendroglia metabolically support axons and contribute to neurodegeneration. *Nature* **487**, 443–448 (2012).
6. Kang, S. H., Fukaya, M., Yang, J. K., Rothstein, J. D. & Bergles, D. E. NG2+CNS glial progenitors remain committed to the oligodendrocyte lineage in postnatal life and following neurodegeneration. *Neuron.* **68**, 668–681 (2010).
7. Yeung, M. S. Y. et al. Dynamics of oligodendrocyte generation and myelination in the human brain. *Cell* **159**, 766–774 (2014).
8. Rivers, L. E. et al. PDGFRA/NG2 glia generate myelinating oligodendrocytes and piriform projection neurons in adult mice. *Nat. Neurosci.* **11**, 1392–1401 (2008).
9. Young, K. M. et al. Oligodendrocyte dynamics in the healthy adult CNS: evidence for myelin remodeling. *Neuron.* **77**, 873–885 (2013).
10. Dimou, L., Simon, C., Kirchhoff, F., Takebayashi, H. & Götz, M. Progeny of Olig2-expressing progenitors in the gray and white matter of the adult mouse cerebral cortex. *J. Neurosci.* **28**, 10434–10442 (2008).
11. Gibson, E. M. et al. Neuronal activity promotes oligodendrogenesis and adaptive myelination in the mammalian brain. *Science* **344**, 1252304 (2014).
12. Scholz, J., Klein, M. C., Behrens, T. E. J. & Johansen-Berg, H. Training induces changes in white-matter architecture. *Nat. Neurosci.* **12**, 1370–1371 (2009).
13. Bengtsson, S. L. et al. Extensive piano practicing has regionally specific effects on white matter development. *Nat. Neurosci.* **8**, 1148–1150 (2005).
14. McKenzie, I. A. et al. Motor skill learning requires active central myelination. *Science* **346**, 318–322 (2014).
15. Xiao, L. et al. Rapid production of new oligodendrocytes is required in the earliest stages of motor-skill learning. *Nat. Neurosci.* **19**, 1210–1217 (2016).
16. Tomassy, G. S. et al. Distinct profiles of myelin distribution along single axons of pyramidal neurons in the neocortex. *Science* **344**, 319–324 (2014).
17. Mensch, S. et al. Synaptic vesicle release regulates myelin sheath number of individual oligodendrocytes in vivo. *Nat. Neurosci.* **18**, 628–630 (2015).
18. Hines, J. H., Ravanelli, A. M., Schwindt, R., Scott, E. K. & Appel, B. Neuronal activity biases axon selection for myelination in vivo. *Nat. Neurosci.* **18**, 683–689 (2015).
19. Gong, S. et al. A gene expression atlas of the central nervous system based on bacterial artificial chromosomes. *Nature* **425**, 917–925 (2003).
20. Kang, S. H. et al. Degeneration and impaired regeneration of gray matter oligodendrocytes in amyotrophic lateral sclerosis. *Nat. Neurosci.* **16**, 571–579 (2013).
21. Holz, A. et al. Molecular and developmental characterization of novel cDNAs of the myelin-associated/oligodendrocytic basic protein. *J. Neurosci.* **16**, 467–477 (1996).
22. Schain, A. J., Hill, R. A. & Grutzendler, J. Label-free in vivo imaging of myelinated axons in health and disease with spectral confocal reflectance microscopy. *Nat. Med.* **20**, 443–449 (2014).
23. Exner, S. *Untersuchungen über die Localisation der Functionen in der Grosshirnrinde des Menschen*. (Braumüller, Vienna, 1881).
24. Hughes, E. G., Kang, S. H., Fukaya, M. & Bergles, D. E. Oligodendrocyte progenitors balance growth with self-repulsion to achieve homeostasis in the adult brain. *Nat. Neurosci.* **16**, 668–676 (2013).
25. Makinodan, M., Rosen, K. M., Ito, S. & Corfas, G. A critical period for social experience-dependent oligodendrocyte maturation and myelination. *Science* **337**, 1357–1360 (2012).
26. Liu, J. et al. Impaired adult myelination in the prefrontal cortex of socially isolated mice. *Nat. Neurosci.* **15**, 1621–1623 (2012).
27. Barres, B. A. et al. Cell death and control of cell survival in the oligodendrocyte lineage. *Cell* **70**, 31–46 (1992).
28. Trapp, B. D., Nishiyama, A., Cheng, D. & Macklin, W. Differentiation and death of premyelinating oligodendrocytes in developing rodent brain. *J. Cell Biol.* **137**, 459–468 (1997).
29. Cerghet, M. et al. Proliferation and death of oligodendrocytes and myelin proteins are differentially regulated in male and female rodents. *J. Neurosci.* **26**, 1439–1447 (2006).
30. Tripathi, R. B. et al. Remarkable stability of myelinating oligodendrocytes in mice. *Cell Rep.* **21**, 316–323 (2017).
31. del Rio Hortega, P. Estudio sobre la neuroglia. Glia escasas ramificaciones (Oligodendroglia). *Bol. Real Soc. Espan. Biol.* **9**, 69–120 (1921).
32. Marques, S. et al. Oligodendrocyte heterogeneity in the mouse juvenile and adult central nervous system. *Science* **352**, 1326–1329 (2016).
33. Murtie, J. C., Macklin, W. B. & Corfas, G. Morphometric analysis of oligodendrocytes in the adult mouse frontal cortex. *J. Neurosci. Res.* **85**, 2080–2086 (2007).
34. Czopka, T., ffrench-Constant, C. & Lyons, D. A. Individual oligodendrocytes have only a few hours in which to generate new myelin sheaths in vivo. *Dev. Cell* **25**, 599–609 (2013).
35. Watkins, T. A., Emery, B., Mulinyawe, S. & Barres, B. A. Distinct stages of myelination regulated by γ-secretase and astrocytes in a rapidly myelinating CNS coculture system. *Neuron.* **60**, 555–569 (2008).
36. Lasiene, J., Matsui, A., Sawa, Y., Wong, F. & Horner, P. J. Age-related myelin dynamics revealed by increased oligodendrogenesis and short internodes. *Aging Cell* **8**, 201–213 (2009).
37. Peters, A. & Kemper, T. A review of the structural alterations in the cerebral hemispheres of the aging rhesus monkey. *Neurobiol. Aging* **33**, 2357–2372 (2012).

38. Yang, G., Pan, F. & Gan, W.-B. Stably maintained dendritic spines are associated with lifelong memories. *Nature* **462**, 920–924 (2009).
39. Chong, S. Y. C. et al. Neurite outgrowth inhibitor Nogo-A establishes spatial segregation and extent of oligodendrocyte myelination. *Proc. Natl Acad. Sci. USA* **109**, 1299–1304 (2012).
40. Redmond, S. A. et al. Somatodendritic expression of JAM2 inhibits oligodendrocyte myelination. *Neuron.* **91**, 824–836 (2016).
41. Shen, S. et al. Age-dependent epigenetic control of differentiation inhibitors is critical for remyelination efficiency. *Nat. Neurosci.* **11**, 1024–1034 (2008).
42. Ouzounov, D. G. et al. In vivo three-photon imaging of activity of GCaMP6-labeled neurons deep in intact mouse brain. *Nat. Methods* **14**, 388–390 (2017).
43. Micheva, K. D. et al. A large fraction of neocortical myelin ensheathes axons of local inhibitory neurons. *eLife* **5**, e15784 (2016).
44. Chang, A., Tourtellotte, W. W., Rudick, R. & Trapp, B. D. Premyelinating oligodendrocytes in chronic lesions of multiple sclerosis. *N. Engl. J. Med.* **346**, 165–173 (2002).
45. Green, A. J. et al. Clemastine fumarate as a remyelinating therapy for multiple sclerosis (ReBUILD): a randomised, controlled, double-blind, crossover trial. *Lancet* **390**, 2481–2489 (2017).

Acknowledgements

We thank M. Pucak, N. Ye, H. Hsieh, and A. Doreswamy for technical assistance; T. Shelly for machining expertise; and members of the Bergles laboratory for discussions. We thank T. McCown (University of North Carolina) for the kind gift of AAV9-MBP-eGFP virus. E.G.H. was supported by a NRSA grant from the NIH (F32NS076098), the Boettcher Foundation, the Whitehall Foundation, the Conrad N. Hilton Foundation (17324), and the National Multiple Sclerosis Society (RG-1701–26733). J.O.M. was supported by a National Multiple Sclerosis Society Postdoctoral Fellowship (FG 2092-A-1) and the Conrad N. Hilton Foundation (17314). A.J.L. was supported by a National Multiple Sclerosis Society Postdoctoral Fellowship (FG 20114-A-1). Funding was provided by grants from the NIH (NS051509, NS050274), the Dr. Miriam and Sheldon G. Adelson Medical Research Foundation, a National MS Society Collaborative Center Award, the Brain Science Institute at Johns Hopkins University, and the Johns Hopkins Medicine Discovery Fund to D.E.B.

Author contributions

E.G.H. and D.E.B. conceived the project, designed the experiments, and wrote the manuscript with input from the other authors. J.O.M. and E.G.H. conducted the sensory manipulation experiments in Figs. 7 and 8 and analyzed data in Fig. 4. J.O.M. contributed to the design of the sensory manipulation experiments, generated Supplementary Fig. 3, and contributed data to Fig. 1 and Supplementary Figs. 4, 6, and 8. A.J.L. conducted and analyzed the viral labeling experiments for Fig. 5. E.G.H. executed and analyzed all other experiments described in the figures, text, and supplementary information.

Competing interests

The authors declare no competing interests.

Additional information

Supplementary information is available for this paper at https://doi.org/10.1038/s41593-018-0121-5.

Reprints and permissions information is available at www.nature.com/reprints.

Correspondence and requests for materials should be addressed to E.G.H. or D.E.B.

Publisher's note: Springer Nature remains neutral with regard to jurisdictional claims in published maps and institutional affiliations.

Methods

Animals. Both female and male mice were used for experiments and were randomly assigned to experimental groups. All mice were healthy and did not display any overt behavioral phenotypes, and no animals were excluded from the analysis. Generation and genotyping of BAC transgenic lines *Mobp-EGFP*[19] (Gensat), *NG2-mEGFP*[24], *Olig2-CreER*[46] and tdTomato reporter mouse line[47] (Ai14, Allen Brain Institute) have been previously described. For experiments using the inducible *Cre–loxP* system to label oligodendrocyte lineage cells, mice were injected with tamoxifen (see "Tamoxifen injection" section below for details). Mice were maintained on a 12-h light/dark cycle, housed in groups no larger than 5, and food and water were provided ad libitum. All animal experiments were performed in strict accordance with protocols approved by the Animal Care and Use Committee at Johns Hopkins University.

In vivo two-photon microscopy. Cranial windows were prepared as previously described[24]. Briefly, mice (2–24 months old) were anesthetized with isoflurane (induction, 5%; maintenance, 1.5–2.0%, mixed with 0.5 L/min O_2), and their body temperature was maintained at 37 °C with a thermostat-controlled heating plate. The skin over the right cerebral hemisphere was removed and the skull cleaned. A 2 × 2 mm region of skull over somatosensory cortex (−0.5 to −2.5 mm from bregma and 2.5 to 4.5 mm lateral) was either thinned (~20 µm thickness) or removed using a high-speed dental drill. For cranial windows, a piece of cover glass (VWR, No. 1) was placed in the craniotomy and sealed with dental cement (C&B Metabond) and a custom metal plate with a central hole was attached to the skull for head stabilization. In vivo imaging sessions began immediately after surgery (thinned-skull preparation) or after a minimum of 3 weeks (chronic cranial window), as noted in the text. During imaging sessions, mice were anesthetized with isoflurane and immobilized by attaching the head plate to a custom stage. Images were collected using a Zeiss LSM 710 microscope equipped with a GaAsP detector using a mode-locked Ti:sapphire laser (Coherent Ultra) tuned to 920 nm. The average power at the sample during imaging was < 30 mW. Vascular landmarks were used to identify the same cortical area over longitudinal imaging sessions. Image stacks were either 425 µm × 425 µm × 100 µm (2,048 × 2,048 pixels; corresponding to cortical layer I) or 425 µm × 425 µm × 550 µm (1,024 × 1,024 pixels; corresponding to layers I–IV) from the cortical surface.

Viral injections. Injection of adeno-associated virus into adult mouse sensory cortex was performed according to standard protocols. Briefly, mice 11–13 weeks old (young cohort) or 52–60 weeks old (middle-aged cohort) were anesthetized using isoflurane (Baxter). Animals were head-mounted in an Angle Two Stereotaxic Instrument (Leica Biosystems) and a microdrill (Ideal) was used to make a burr hole through the skull. The injection was targeted to sensory cortex, at 1.0 mm posterior to bregma, 3.0 mm lateral, and 100 nm depth into the cortex. We injected 1×10^9 viral genomes of AAV9-MBP-eGFP (a kind gift from T. McCown) were injected using a Nanoject (Drummond Scientific) at 23 nL per s. At least 21 days after the injection, animals were perfused and tissue was collected for immunohistochemistry.

Immunohistochemistry. Mice were deeply anesthetized with sodium pentobarbital (100 mg/kg b.w.) and perfused transcardially with 4% paraformaldehyde (PFA in 0.1 M phosphate buffer, pH 7.4). For horizontal sections, cortices were flat-mounted between glass slides and postfixed in 4% PFA overnight at 4 °C, transferred to 30% sucrose solution (in PBS, pH 7.4), and stored at 4 °C for more than 48 h. Brains were extracted, frozen in TissueTek, sectioned (coronal, bregma 0.2 to −1.9 mm; horizontal, 0–1 mm) at 30–50 µm thick. Immunofluorescence was performed on free-floating sections. Sections were preincubated in blocking solution (5% normal donkey serum, 0.3% Triton X-100 in PBS, pH 7.4) for 1 or 2 h at room temperature, then incubated for 2 days at 4 °C in primary antibody (listed along with secondary antibodies in Supplementary Table 1). Secondary antibody incubation was performed at room temperature for 2–4 h. Sections were mounted on slides with ProLong antifade reagent (Invitrogen). Images were acquired using either an epifluorescence microscope (Zeiss Axio-imager M1) with Axiovision software (Zeiss) or a confocal laser-scanning microscope (Zeiss LSM 510 Meta; Zeiss LSM 710).

Sensory enrichment. For sensory enrichment, mice were placed in standard mouse cages containing a grid of strings of beads spaced 1.5 to 3 cm apart and a tolerance of 1 cm positional movement for 3 weeks over both light and dark cycles[38]. For sensory deprivation, left-side whiskers were completely removed every 2–3 d for 3 weeks. Mice were anesthetized with isoflurane for whisker removal (or mock whisker removal with anesthesia for control). The same baseline region of contralateral somatosensory barrel cortex was re-imaged after 3 weeks for either control (standard cage ± isoflurane exposure every 2–3 d), sensory enrichment, sensory deprivation, or a combination of sensory deprivation and enrichment conditions.

Image processing and analysis. Image stacks and time-series were analyzed using FIJI/ImageJ. All analysis was performed on unprocessed images except for middle-aged myelin sheath analysis images. For presentation in figures, image brightness and contrast levels were adjusted for clarity. Myelin sheath images were additionally processed with a Mean filter (radius = 2 pixels) to denoise. For the pseudocolor display of individual myelin sheaths (Figs. 6 and 7), a three-dimensional region of interest was defined for each timepoint and a custom-written FIJI script was used to segment and/or colorize the sheath. Longitudinal image stacks were registered using FIJI plugins 'Correct 3D drift'[48] or 'PoorMan3DReg', and then randomized for analysis by a blinded observer.

Cell tracking. Cells were followed in three dimensions using custom FIJI scripts by defining EGFP$^+$ cell bodies at each timepoint, recording *xyz* coordinates, and defining cellular behavior (new, dying, proliferating, differentiating, or stable cells). OPC migration, proliferation, death, and differentiation were defined as previously described[24]. Briefly, OPCs were classified as proliferating if two cells appeared in the same location and cell bodies were separated by less than 50 µm. Dying OPCs displayed a shortening and blebbing of processes and a complete disappearance of EGFP (*NG2-mEGFP*) and tdTomato (*Olig2-CreER;R26-lsl-tdTomato*) fluorescence simultaneously (Supplementary Fig. 4). Differentiating OPCs exhibited morphological changes classically associated with oligodendrocyte differentiation, including a progressive decrease in EGFP (*NG2-mEGFP*) fluorescence and sustained tdTomato (*Olig2-CreER;R26-lsl-tdTomato*) fluorescence (Fig. 2). Differentiating OPCs that died before integrating as mature oligodendrocytes lost EGFP fluorescence, had radial, highly branched processes characteristic of premyelinating oligodendrocytes and abruptly lost tdTomato fluorescence. TdTomato$^+$ cell fragments were occasionally observed in the vicinity of the original cell (Fig. 2e,f).

Myelin sheath analysis. In vivo *z*-stacks collected from *Mobp-EGFP* mice were acquired using two-photon microscopy. *Z*-stacks from middle-aged mice were background-subtracted and processed with a 0.5- to 1-pixel median filter to aid in the identification of myelin internodes. All myelin sheaths that terminated within a volume of 125 × 125 × 50 µm^3 from the pial surface were traced in FIJI using Simple Neurite Tracer[49] and identified as continuous, interrupted, or isolated. Continuous sheaths have nodes of Ranvier on either side (abutting two other sheaths). Interrupted sheaths are bordered by only one node of Ranvier, and the other end of the sheath extends along a bare segment of axon. Isolated sheaths are bordered by bare axon on either side. Myelin sheaths within the field that extended beyond the imaged area or could not be definitively identified were classified as 'undefined'. Myelin paranodes were identified by increased EGFP fluorescence intensity (Fig. 1). Nodes of Ranvier were identified by plotting an intensity profile across the putative node; if the intensity decreased to zero between the adjacent oligodendrocyte processes, and the length of the gap between EGFP$^+$ processes was < 5 µm, the structure was considered a node[50]. For each field, myelin sheaths were traced by one investigator and independently assessed by a second investigator.

Myelin sheath analysis of individual oligodendrocytes. Confocal *z*-stacks of virally infected, EGFP$^+$ oligodendrocytes were acquired at 40×, using an oil immersion objective on a Zeiss 510 microscope. Myelin sheaths were traced in Imaris (Bitplane) to quantify the number of myelin sheaths per oligodendrocyte and to categorize each myelin sheath as isolated (no adjacent myelin sheaths), interrupted (one adjacent myelin sheath), continuous (two adjacent myelin sheaths), or undefined (cut by the sectioning plane so that adjacent myelin sheaths could not be determined). The length of each myelin sheath was also quantified. Because isolated GFP$^+$ oligodendrocytes were chosen for this analysis, all GFP$^+$ myelin sheaths in close proximity (less than ~50 µm) to a GFP$^+$ oligodendrocyte cell body were considered connected to that oligodendrocyte.

Tamoxifen injections. Tamoxifen (Sigma; T5648–1G; CAS:10540–29–1) was weighed and dispersed in sunflower seed oil (Sigma; S5007; CAS: 8001–21–6) for a final concentration of 10 mg/mL. The solution was vortexed vigorously and then sonicated for 5 min. This cycle was repeated three to four times, until tamoxifen was completely dissolved. The tamoxifen/oil emulsion was stored at 4 °C, protected from light, and used for a maximum of 7 d. Mice 4 weeks old were injected intraperitoneally with 100 mg/kg bodyweight of the tamoxifen/oil emulsion once per day for 5 consecutive days to induce Cre recombination.

Statistics and reproducibility. No statistical methods were used to predetermine sample sizes, but our sample sizes are similar to those reported in previous publications. Data analysis was performed blind to the conditions of the experiments. Statistical analyses were performed with Origin Pro (OriginLab) or Excel (Microsoft). All datasets were tested with the Shapiro–Wilk test to determine normality. Significance was determined using unpaired two-tailed Student's *t* tests or one-way ANOVA with Tukey post hoc tests. Each figure legend contains the statistical tests used to measure significance and the corresponding significance level (*P* value). *N* values represent the numbers of animals used in each experiment. Data are reported as mean ± s.e.m., and $P < 0.05$ was considered statistically significant.

Antibody validation. Antibody source, dilution, catalog number, and unique identifier are listed in Supplementary Table 2. Antibodies were selected according

to the antibody validation profiles reported by the distributing companies and in publications. Noncommercial antibodies (anti-Caspr and anti-NG2 antibodies) were selected according to validation profiles reported in publications and are specifically referenced by the citation and PMID.

Life Sciences Reporting Summary. Mouse lines used in this study are listed in Supplementary Table 1. Ages of the experimental animals are listed in corresponding figure legends. Further information on experimental design is available in the Life Sciences Reporting Summary.

Data availability. All data that support the findings, tools, and reagents will be shared on an unrestricted basis; requests should be directed to the corresponding authors.

Code availability. All published code will be shared on an unrestricted basis; requests should be directed to the corresponding authors.

References

46. Takebayashi, H. et al. The basic helix-loop-helix factor olig2 is essential for the development of motoneuron and oligodendrocyte lineages. *Curr. Biol.* **12**, 1157–1163 (2002).
47. Madisen, L. et al. A robust and high-throughput Cre reporting and characterization system for the whole mouse brain. *Nat. Neurosci.* **13**, 133–140 (2010).
48. Parslow, A., Cardona, A. & Bryson-Richardson, R. J. Sample drift correction following 4D confocal time-lapse imaging. *J. Vis. Exp.* **85**, e51086 (2014).
49. Longair, M. H., Baker, D. A. & Armstrong, J. D. Simple Neurite Tracer: open source software for reconstruction, visualization and analysis of neuronal processes. *Bioinformatics* **27**, 2453–2454 (2011).
50. Koudelka, S. et al. Individual neuronal subtypes exhibit diversity in cns myelination mediated by synaptic vesicle release. *Curr. Biol.* **26**, 1447–1455 (2016).

nature research

Corresponding author(s): Bergles/Hughes

☐ Initial submission ☐ Revised version ☒ Final submission

Life Sciences Reporting Summary

Nature Research wishes to improve the reproducibility of the work that we publish. This form is intended for publication with all accepted life science papers and provides structure for consistency and transparency in reporting. Every life science submission will use this form; some list items might not apply to an individual manuscript, but all fields must be completed for clarity.

For further information on the points included in this form, see Reporting Life Sciences Research. For further information on Nature Research policies, including our data availability policy, see Authors & Referees and the Editorial Policy Checklist.

Experimental design

1. Sample size

Describe how sample size was determined.

No statistical methods were used to pre-determine sample sizes but our sample sizes are similar to those reported in previous publications.

2. Data exclusions

Describe any data exclusions.

No data points are excluded from our analyses and figures.

3. Replication

Describe whether the experimental findings were reliably reproduced.

All attempts at replication were successful.

4. Randomization

Describe how samples/organisms/participants were allocated into experimental groups.

Both female and male mice were used for experiments and were randomly assigned to experimental groups as reported in methods section, "Mice".

5. Blinding

Describe whether the investigators were blinded to group allocation during data collection and/or analysis.

Longitudinal image stacks were registered and then randomized for analysis by a blinded observer as reported in the methods section, "Image processing and analysis".

Note: all studies involving animals and/or human research participants must disclose whether blinding and randomization were used.

6. Statistical parameters

For all figures and tables that use statistical methods, confirm that the following items are present in relevant figure legends (or in the Methods section if additional space is needed).

n/a	Confirmed
☐	☒ The exact sample size (*n*) for each experimental group/condition, given as a discrete number and unit of measurement (animals, litters, cultures, etc.)
☐	☒ A description of how samples were collected, noting whether measurements were taken from distinct samples or whether the same sample was measured repeatedly
☐	☒ A statement indicating how many times each experiment was replicated
☐	☒ The statistical test(s) used and whether they are one- or two-sided (note: only common tests should be described solely by name; more complex techniques should be described in the Methods section)
☐	☒ A description of any assumptions or corrections, such as an adjustment for multiple comparisons
☐	☒ The test results (e.g. *P* values) given as exact values whenever possible and with confidence intervals noted
☐	☒ A clear description of statistics including central tendency (e.g. median, mean) and variation (e.g. standard deviation, interquartile range)
☐	☒ Clearly defined error bars

See the web collection on statistics for biologists for further resources and guidance.

Software

Policy information about availability of computer code

7. Software

Describe the software used to analyze the data in this study.	Origin Pro 2016 (OriginLab), Excel 2016 version 15.27 (Microsoft), FIJI (ImageJ), Imaris (Bitplane)

For manuscripts utilizing custom algorithms or software that are central to the paper but not yet described in the published literature, software must be made available to editors and reviewers upon request. We strongly encourage code deposition in a community repository (e.g. GitHub). *Nature Methods* guidance for providing algorithms and software for publication provides further information on this topic.

Materials and reagents

Policy information about availability of materials

8. Materials availability

Indicate whether there are restrictions on availability of unique materials or if these materials are only available for distribution by a for-profit company.	All published code, tools, and reagents will be shared on an unrestricted basis.

9. Antibodies

Describe the antibodies used and how they were validated for use in the system under study (i.e. assay and species).	Antibody source, dilution, catalog number, and unique identifier are listed in Supplementary Table 2. Antibodies were selected according to the antibody validation profiles reported by the distributing companies and in publications. Noncommercial antibodies (anti-Caspr and anti-NG2 antibodies) were selected according to validation profiles reported in publications and are specifically referenced by the citation and PMID.

10. Eukaryotic cell lines

a. State the source of each eukaryotic cell line used.	No eukaryotic cell lines were used.
b. Describe the method of cell line authentication used.	No eukaryotic cell lines were used.
c. Report whether the cell lines were tested for mycoplasma contamination.	No eukaryotic cell lines were used.
d. If any of the cell lines used are listed in the database of commonly misidentified cell lines maintained by ICLAC, provide a scientific rationale for their use.	No eukaryotic cell lines were used.

Animals and human research participants

Policy information about studies involving animals; when reporting animal research, follow the ARRIVE guidelines

11. Description of research animals

Provide details on animals and/or animal-derived materials used in the study.	Mouse lines used in this study are listed in Supplementary Table 1. Age of the experimental animals is listed in corresponding figure legends.

Policy information about studies involving human research participants

12. Description of human research participants

Describe the covariate-relevant population characteristics of the human research participants.	This study did not involve human research participants.